Analysis of Antenna Manufacturing Methods: Addressing Challenges in 3D Printing

Caleb Keathley*, Bibek Kattel, Winn Elliott Hutchcraft*, and Richard Gordon
Electrical and Computer Engineering
University of Mississippi
Oxford, MS, USA
*Email: caleb.keathley@rtx.com, eeweh@olemiss.edu

***Abstract*—This study discusses the design and fabrication process of a bowtie antenna using a traditional milling method and a 3D printing method. The various parameters related to the manufacturing process are discussed, and their effect on the design process is highlighted. Both a milled antenna and a fully 3D printed antenna were fabricated and the design and manufacturing process of the two antennas was compared. This paper particularly focuses on the intricacies of antenna design through 3D printing. The objective of the research is to compare and contrast the two fabrication processes and highlight the challenges associated particularly with using 3D printing technology. The improvement of these shortcomings helps to mature 3D printing technology and work toward improvements for future electromagnetic applications.**

***Index Terms*—3D printing, bowtie antenna, challenges, manufacturing method, milling, PETG, printed antenna**

I. Introduction

Computerized Numerical Control (CNC) milling and 3D printing methods are widely recognized techniques utilized in the fabrication of planar antennas. The milling process functions as a subtractive method, eliminating undesired materials, whereas 3D printing operates as an additive process, depositing materials to formulate the required structure. Milling has been extensively studied and is considered a more mature technology than 3D printing [1]. At present, milling boasts superior surface finish, broader ranges of material choices, higher precision, and, in many cases, yields components with greater structural strength compared to 3D printing processes [2], [3]. Conversely, 3D printing provides enhanced design and fabrication flexibility, rapid prototyping capabilities, and minimizes material waste [4]–[6]. In addition to being a recent innovation and having a flexible process, the limitations of 3D printing can be refined, positioning it as a more efficient and potent technique for antenna design in the future. The fabrication of antennas with complex geometries using additive manufacturing processes has been explored in [7]. Additionally, studies have identified the potential of implementing novel 3D printed antennas for significant advancements in various fields including space communications, 5G applications, and Millimeter-Wave Applications [8]–[10].

The 3D printing procedure commences with creating a computer model of the antenna. Subsequently, the computer model is imported into the 3D printing software. The appropriate filament material is then used in the 3D printer to fabricate the computer model. Despite the apparent simplicity of this process, challenges arise when executing a 3D printing process. Although certain challenges have been highlighted in [11], [12], this paper further explores the practical impediments encountered specifically in employing this technology for the design and fabrication of a bowtie antenna.

The objective of this study is to compare the design and manufacturing processes of a bowtie antenna using milling and 3D printing methods. This study places particular emphasis on the intricacies of antenna design through the 3D printing process. This paper highlights the array of challenges encountered during the manufacturing process and provides insights into the methods used by the authors to overcome these hurdles. These insights can prove invaluable to researchers involved in antenna design utilizing 3D printing technology. The resolution of such difficulties in the 3D printing process has the potential to progress the maturity and effectiveness of this technology, further solidifying its role as a powerful tool for creating intricate electromagnetic devices in the future.

II. Methodology

In this study, the design objective was to fabricate an antenna operating at 1.5 GHz with a few constraints on the design, particularly, a maximum width of less than 70 mm. Given both this physical limitation and a requirement to feed the antenna in a certain way, an unconventional bowtie configuration was chosen such that the bowtie element is rotated by 90^o. The use of this type of antenna is presented in an antenna array in [13]. This paper utilized the design of a single element of the array for 1.5 GHz frequency operation. The antenna's geometry was first modeled in CST Microwave Studio, employing variables to optimize each dimension. The antenna design specifications for this antenna were not previously defined, so numerous parametric sweeps and simulations were employed to determine the antenna dimensions. Figure 1 illustrates the CST software model of the milled bowtie antenna, with copper depicted in yellow and the substrate in blue. Another notable departure from conventional designs is the incorporation of a partial ground plane on the antenna's reverse side as shown in Fig. 2, adding additional complexity to the manufacturing process as both sides require milling or 3D printing compared to designs with a full ground plane.

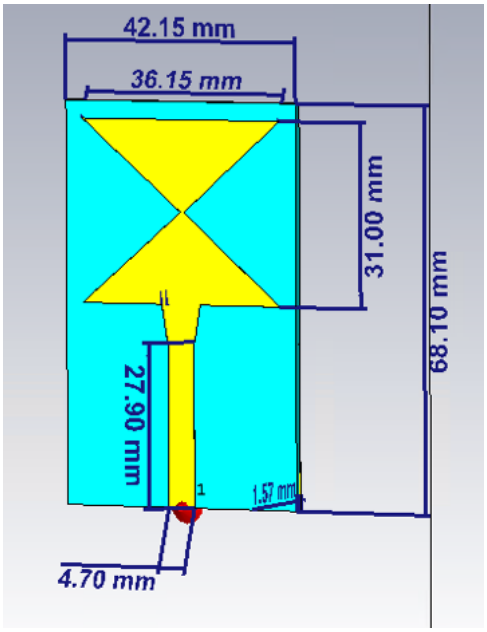

Fig. 1. CST model of the bowtie antenna, From [14].

The substrates necessary for milling, such as RT Duroid boards, were only available in fixed thicknesses and dielectric constants, necessitating fixing the substrate thickness and dielectric constant at predefined values in the CST models for the milling design. In contrast, 3D printing offers flexibility in adjusting additional parameters, such as substrate thickness and dielectric constant values. Consequently, a separate simulation was conducted for the 3D printed antenna within the software incorporating the additional design variables and optimizations. Due to the use of the substrate thickness as a design parameter, the 3D printed antenna is designed with differing geometric values than the milled antenna.

A. Traditional Milling Process

With the simulated design finalized, the subsequent step involved fabricating the antenna using a milling machine. Each layer of the antenna was exported from simulation software in .dxf format, resulting in a file for the top layer, substrate layer, and ground plane layer. These files were then processed using CircuitCam, software for the milling machine path calculation and tool bit assignment. The processed job file is exported into BoardMaster, the software interfacing directly with the milling machine. Once the substrate board was aligned on the milling base, the milling process on the LPKF machine was initiated. Notably, the bowtie antenna design required milling on both sides of the substrate, necessitating a horizontal flip after the initial side had been milled. The guidelines on the milling process have been detailed in [14].

The specific substrate material utilized for milling the antennas on the LPKF machine was "RT/duroid 5870", characterized by a thickness of 1.57 mm and a dielectric constant of 2.33. To facilitate measurement on a network analyzer, a SubMiniature version A (SMA) port was soldered to the microstrip and ground plane. The milled antenna, post-SMA port soldering, is depicted in Fig. 2.

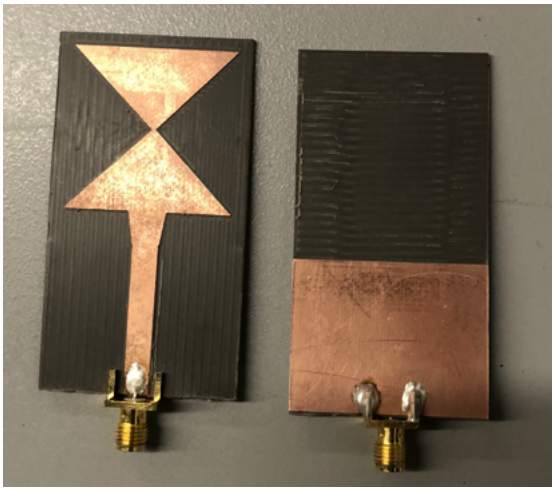

Fig. 2. Milled bowtie antenna, From [14].

B. 3D Printing Process

For additive manufacturing, a commercial tabletop nScrypt 3D printer was employed. The antenna's substrate was constructed using PETG, a widely used commercial filament material. The metallic layer was composed of silver ink manufactured by Voltera [15]. The nScrypt printer featured two separate extruder nozzles for the dielectric filament and the silver ink. The filament material was heated and extruded through a narrow ceramic tip with an inner diameter of 125 μm whereas the silver ink was extruded utilizing a 23 gauge metal tip.

The antenna designed using the simulation software was exported as STL files separately for the substrate and metallic layers of the antenna. This allowed for the separate fabrication of these layers by the 3D printer. It is important to note that, unlike the two-dimensional dxf files needed for the milling machine, the nScrypt machine operates in three dimensions and thus requires three-dimensional STL files. For a thorough understanding of the 3D printing process, a detailed explanation can be found in [14]. The antenna manufactured by using the 3D printing process is presented in Fig. 3.

III. Results

The fabricated antennas were measured using an Agilent PNA X which was calibrated with an 85052D calibration kit. The calibration standard uses a short, open, and broadband load (SOL) to calibrate the Vector Network Analyzer (VNA) port used for the antenna measurements [16].

The results for the antenna measurements are presented in Figure 4 and provide a comparison between the simulated and the fabricated antennas. Both fabricated antennas demonstrate a return loss better than -8 dB at the targeted 1.5 GHz frequency. Notably, there is a discernible frequency shift of 230 MHz between the simulated and measured frequency

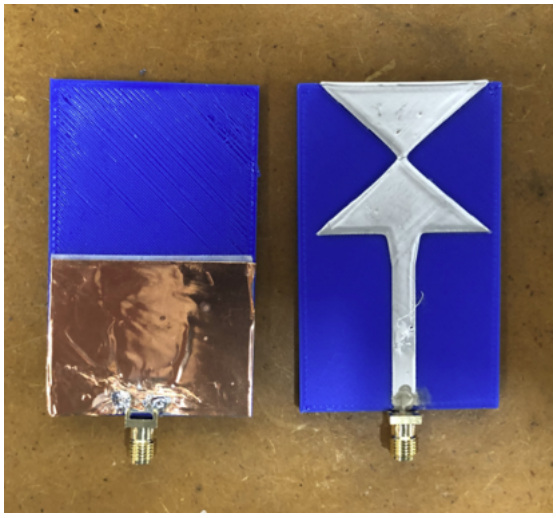

Fig. 3. Fully 3D printed bowtie antenna, From [14].

resonance. While the initial concern centered on potential manufacturing errors in the fabricated antennas, it was observed that multiple antennas exhibited a similar 230 MHz discrepancy between the CST simulations and the actual fabricated antennas. The prevailing hypothesis is that this resonance shift of 230 MHz represents a modeling error in the CST simulations. This assertion is supported by the fact that both the milled and 3D printed antennas exhibit peak resonances displaced by the same amount from their respective simulations.

The milled and 3D printed CST simulations show slight differences in Fig. 4 due to the thickness parameter used to optimize the 3D printed antenna. The antennas fabricated using both methodologies exhibit nearly identical operating frequencies, with the 3D printed antenna showing a slightly deeper resonance. However, a key observation is the disparity between the results of simulated and fabricated antennas, likely stemming from potential modeling errors in the CST simulations and issues with the measurements related to the

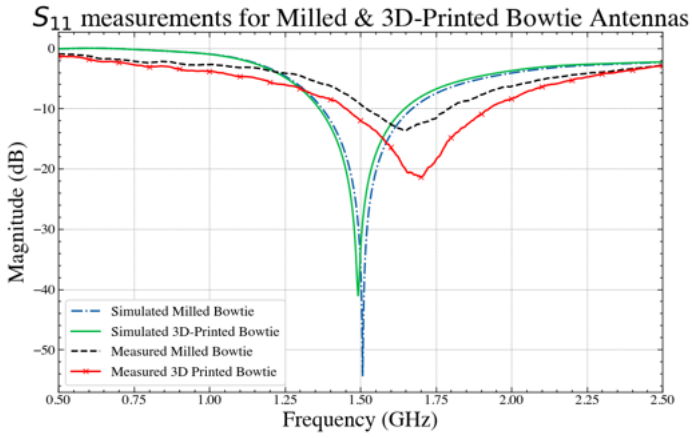

Fig. 4. S_{11} measurements results.

feeding mechanism.

IV. Challenges Encountered in 3D Printing

Although the 3D printing technology presents numerous possibilities for antenna design, its infancy is accompanied by various challenges. 3D printing involves a multitude of critical parameters such as each layer's thickness, extrusion width, extrusion temperature, bed temperature, print speed, infill density, and infill pattern that all necessitate optimization to produce a high-quality print [12], [17]. A few of the key challenges and limitations that were faced in the course of this study have been presented in the subsequent subsections.

Material Selection and Characterization: The availability of various material choices for 3D printing filaments is expanding but many of these filaments lack comprehensive data on their respective permittivity and dielectric loss, both of which are critical parameters in antenna design. Despite an increase in available filaments, many common 3D printing filaments have very low permittivity limiting their use in antenna design and other RF applications. For instance, during the time of the antenna fabrication, the dielectric properties of the PETG used in this study had not been characterized. Therefore we relied on the prior experience of a research group working with PETG and used a permittivity value of 2.75. However, when the PETG was later measured, the relative permittivity of the PETG was determined to be 2.50 [6].

Bed Balancing and Manual Z-Height Adjustments: Achieving successful 3D prints necessitates precise bed balancing. This entails ensuring the bed is meticulously aligned in the horizontal x-y plane. If the bed is not properly balanced, there is a chance the printer head will crash and consequently damage the print in progress while moving in the x-y direction. Additionally, it is imperative to manually adjust the distance between the extruder's tip and the print bed which is defined by the Z-height. This adjustment verifies that the print tip is in close proximity to the bed without actually making contact. If the distance is too large, the filament may not adhere adequately, potentially leading to clogging of the extruder tip. Conversely, if the print tip is too close to the bed, there is a risk of collision, which could result in damage to both the extruder tips and the bed. This manual adjustment process demands a high degree of skill and precision but is crucial for achieving accurate and consistent print outcomes. In our prints, we maintained a gap equivalent to the thickness of a piece of paper between the print head and the print bed, utilizing the built-in camera of the 3D printer for manual Z-height adjustment, as depicted in Fig. 5.

Bed Adhesion: Ensuring the initial filament layers adhere securely to the 3D printer bed is a critical aspect of the 3D printing process. In this study, for improved adhesion of the substrate filament to the 3D printer bed, a Polyetherimide (PEI) sheet was applied to the bed [18]. Once the printed substrate and the printer bed cool, the substrate can detach with minimal force from the bed, complicating the subsequent ink-printing step. To address this challenge, painter's tape was employed to hold the substrate layer to the bed before printing

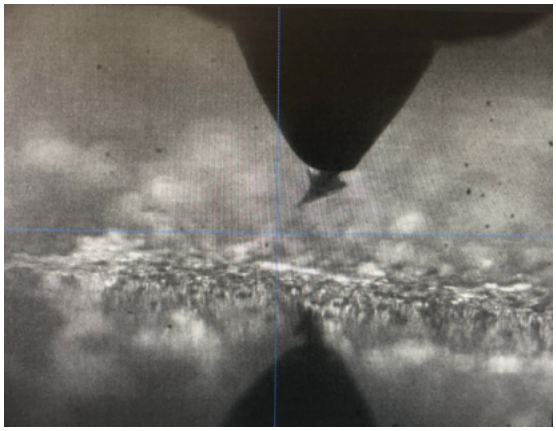

Fig. 5. Extruder tip with manual z-height adjustment process, From [14].

the ink layer. While effective, this solution can introduce offset errors into the ink printing if not executed with precision. Additionally, when the substrate surface is no longer perfectly flat, as is the case after printing the bowtie element layer, printing the ground plane accurately becomes increasingly difficult. Consequently, for the 3D printed antenna, copper tape was chosen for the ground plane over printing silver ink as seen in Fig. 3 to mitigate these challenges.

***Substrate Warping**:* One of the primary challenges was managing substrate warping during the printing process as explained in [19]. This phenomenon can distort the intended antenna geometry, potentially compromising its performance characteristics. We found that this issue usually occurred when base layers of the printed substrate contracted due to inadequate bed temperature. To solve this issue, a good balance of the filament extrusion speed, extruder temperature, bed temperature, layer height as well a proper bed adhesion was required [5]. An example of substrate warping during the antenna fabrication is shown in Fig. 6.

***Nozzle Maintenance**:* Ensuring the nozzle extruder and smart pump remain free of obstructions and function optimally is a critical aspect of the printing process. Issues such as clogging as seen in Fig. 7 can lead to sub-optimal print quality and performance. Between each substrate layer, the filament retracts into the feed to stop the flow while the print bed reorients to the next layer's starting position. The configurable settings for Z-retraction are distance retracted and speed of retraction. If either setting is incorrect, the filament and ink can either leak on the previous layer during reorientation or clog in the extruder. Managing Z-retraction settings is vital for avoiding unwanted smearing, and fine-tuning this parameter is

Fig. 6. Substrate warping.

Fig. 7. Filament overflow due to nozzle clog.

crucial for achieving high-quality results.

***Metal layer printing**:* Although substrate printing has advanced significantly using 3D printing, advancement in printing the metallic layer has lagged behind. Unlike the solid filament material used for printing the dielectric layer, the metallic inks are in a semisolid state and need to be preserved at cold temperatures during storage. They are usually available in a syringe or must be syringed and dispensed using air pressure. However, this method has a few issues. First, the flow of the ink is not uniform due to its high viscosity, causing it to stick to the syringe wall, resulting in an irregular flow. This can result in an uneven flow and create gaps between stripes or dispense clumps as shown in Fig. 8. For our 3D printed antenna, the printed ink layer was not uniform with some noticeable ridges as seen in Fig. 9. This reduced the dimensional accuracy of the printed layer, and the 3D printing method was seen to have more fabrication inconsistencies compared to the milling method as in [3]. Second, because of the high viscosity, it is difficult to extrude the ink through a very thin nozzle. Hence we had to switch to a nozzle of about 0.68 mm for extruding the ink compared to $125\,\mu\mathrm{m}$ used for the dielectric filament. Additionally, the ink necessitates a long duration to dry and cure which is a challenge when both sides of the antenna require ink deposition. Finally, the ink is rather expensive and has a short shelf life increasing the cost of experimentation.

***Print Time**:* The time required for printing is a significant consideration, especially in industrial applications where effi-

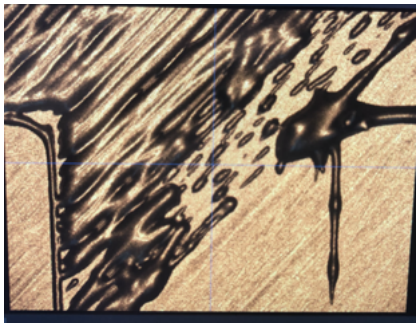

Fig. 8. Uneven ink deposit.

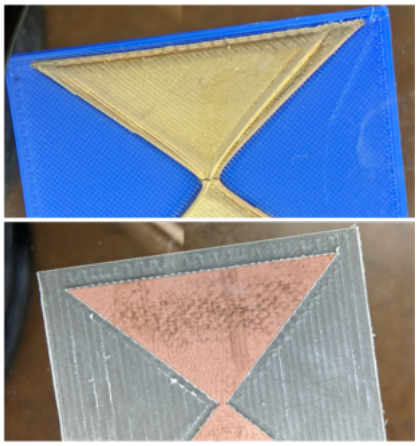

Fig. 9. Zoomed view of the bowtie element of the two antennas.

ciency is paramount. The printing speed directly correlates with various parameters including the size of the ceramic filament feed tips, print speed, extrusion width, substrate size, and complexity of the infill pattern [17]. During the initial substrate printing attempts, a much slower speed was used which had prints taking about 5 hours to complete. Having the printer remain consistent in flow and quality for 5 hours was nearly impossible. After increasing the filament extrusion past the manufacturer's recommended speed for the ceramic tips, we had much-improved success with the extruder's flow rate and subsequently substrate print stability. Currently, 3D printing an antenna takes approximately 24 hours to complete mainly due to the substrate cooling and the silver nitrate ink curing. In contrast, the milled antenna was fully milled within one hour.

SMA Connector Attachment: In contrast to traditional milling, which allows for the use of soldering to attach the SMA connector, the sensitivity of the silver nitrate ink to high temperatures precludes this method. Hence, this study adopted an alternative approach, coating multiple layers of highly conductive silver paste ink over the SMA pin to attach it to the 3D printed ink layer of the antenna as shown in Fig. 3. However, this method requires a long curing time. Additionally, it is worth noting that this alternative is costly and prone to damage in comparison to soldering.

Standardization of Software: Different 3D printers utilize proprietary software and employ varying methods for slicing each substrate layer. Consequently, certain infill patterns may be exclusive to specific printers. Even when employing the same infill pattern for printing a structure on printers from different manufacturers, there is a high likelihood of variations in the structural parameters. This underscores the importance of utilizing standardized software, particularly for the slicing operation, to generate consistent infill density and pattern, as emphasized in [17].

Comparative Cost Analysis: The manufacturing cost of antennas using 3D printing remains notably higher than that of its traditional milling counterpart. Even excluding the cost of the 3D printer itself, the silver nitrate ink utilized for the metallic structure of an antenna proves to be considerably more expensive than prefabricated dielectric substrates. Additionally, consumable parts such as 3D printer tips incur relatively higher expenses compared to the drill bits used in milling machines. The time and effort required to successfully 3D print an antenna are significantly more when compared to milling an antenna. However, as the 3D printing process matures, these issues will likely be significantly reduced.

V. Discussion

The findings of this study underscore the distinctive advantages of both milled and 3D printed antennas, each of which excels in specific applications. The milled antenna, characterized by a streamlined design process with fewer parameters, emerges as a cost-effective manufacturing option. Its simplicity facilitates mass production, providing a consistent and economical solution. In contrast, the 3D printed antenna offers a multitude of adjustable parameters all available in the design process, presenting a more intricate approach, albeit beneficial for research and experimentation. A notable advantage of 3D printing lies in the capability to vary substrate thickness and permittivity using lower infill density [6] during the design process, enabling comprehensive parametric sweeps in CST simulations for optimizing antenna designs.

The 3D printer filament feed was much smaller than the milling machine drill bit which should result in more accurate fabricated antennas compared to the milled fabricated antennas. However, in practice, we observed that the 3D printing process has less dimensional accuracy than the milling process. This issue became evident when the printed ink layer displayed non-uniformity, resulting in noticeable ridges, as illustrated in Fig. 9. The unevenness of the printed layer diminished its dimensional accuracy. Consistent with findings in [3], we noted that the 3D printing method also introduces more fabrication inconsistencies compared to the milling process.

Despite its promising capabilities, the 3D printing process also comes with challenges as mentioned in the previous sections. 3D printing technology is in its infancy, demanding meticulous adjustments and detail to generate desired 3D prints. The process involves numerous small components and completing a print entails overcoming a steep learning curve. Additionally, the post-printing cleanup is notably tedious. The novelty of the technology results in the absence of comprehensive and established documentation. A case in point is the maintenance of the filament feed nozzle. As explained in [14], the ceramic tips enclosure needs to be torqued at room temperature prior to heating to 240°C (for PETG). However, once the heater ring reaches the target temperature, the enclosure has loosened, a subtle issue not immediately apparent to users. The loose parts cause material overflow, coating the ceramic extruder tip and causing potential damage and increased wear, as illustrated in Fig. 7. The solution to this issue is to torque the enclosure again once the heater ring reaches the desired temperature. While learning through experimentation can lead to a deep understanding of the 3D printer, trial and error also contribute to increased time for

prints as well as the risk of damaging the machine hardware, 3D printer consumables, and printing materials.

VI. Conclusion and Future Work

This study has conducted a comprehensive analysis of the design and manufacturing processes for a bowtie antenna using both milling and 3D printing methods. The selection between these methods is contingent upon the specific requirements of the antenna design. 3D printing offers significantly more versatility, enabling a wider array of design options and optimizations. 3D printing is able to incorporate varying levels of thickness and permittivity as design parameters as elucidated in this paper. This facilitates the simulation and design processes for 3D printed antennas, particularly for research and experimental purposes.

There are three main areas of improvement for this study: characterization of the substrate, geometric fabrication error, and simulation discrepancy. The first area of improvement is to increase the accuracy of the dielectric constant in the CST Simulation models by calculating the relationship between infill density and the dielectric constant of the PETG substrate. The 3D printed antenna measured results show a peak resonance frequency that was higher than the milled antenna measured results. In contrast, the simulation results predicted that the 3D printed antenna would have a lower peak resonance than the milled antenna. The resonance discontinuity between the simulation and measured antenna results is justified by the inaccurate dielectric constant value used in the CST simulation.

To bolster the geometric accuracy of both the milling machine and 3D printed antennas, the first step is to measure the current errors. The next step would be to use varying tools namely smaller drill bits for the milling machine and smaller ceramic tips for the filament feed extruder to minimize these errors and obtain better accuracy. However, both smaller drill bits and ceramic tips greatly complicate the fabrication process and would require a complete retesting of the milling machine and 3D printer settings.

The final area of improvement is to determine the cause of the discrepancies between simulation and fabrication. The 230 MHz shift is presumed to be due to a measurement port error. One solution to help determine the simulation and fabrication discontinuity would be to simulate both the fabricated antennas using the measured dimensions. CST simulations are easier to adjust than completely fabricating a new antenna, and while verification simulations may not operate at the targeted frequency resonance, the verification simulations would quickly reveal the expected results of the fabricated antennas.

Our future research endeavors will seek to establish metrics for analyzing the cost and scalability of antenna design using both the milling and 3D printing methods. Additionally, we will focus on addressing and overcoming the challenges associated with 3D printing to fabricate 3D printed antennas with improved performance. This includes exploring methods to improve the permittivity of commonly available 3D printing filaments by compounding them with nanoparticles materials [20]. This paper offers valuable insights for researchers engaged in antenna design using 3D printing technology by highlighting the challenges encountered during the 3D printing process and presenting viable solutions to overcome them. Addressing these challenges is paramount for advancing the maturity and efficacy of 3D printing.

Acknowledgement

We thank Dwight O'Dell for his immense support in setting up CST servers and fabrication of the antennas. This work was supported in part by Raytheon Co. and the NSF Industry University Cooperative Research Centers under Grant 1822104.

References

[1] B. Z. Balázs, N. Geier, M. Takács, and J. P. Davim, "A review on micro-milling: Recent advances and future trends," *The International Journal of Advanced Manufacturing Technology*, vol. 112, pp. 655–684, 2021.

[2] Protolabs Network. "3D printing vs. CNC machining." (Dec. 13, 2023), [Online]. Available: https://www.hubs.com/knowledge-base/3d-printing-vs-cnc-machining/.

[3] M. Ferrando-Rocher, J. I. Herranz-Herruzo, A. Valero-Nogueira, and B. Bernardo-Clemente, "Performance assessment of gap-waveguide array antennas: CNC milling versus three-dimensional printing," *IEEE Antennas and Wireless Propagation Letters*, vol. 17, no. 11, pp. 2056–2060, 2018. DOI: 10.1109/LAWP.2018.2833740.

[4] D. Helena, A. Ramos, T. Varum, and J. N. Matos, "Antenna design using modern additive manufacturing technology: A review," *IEEE Access*, vol. 8, pp. 177 064–177 083, 2020. DOI: 10.1109/ACCESS.2020.3027383.

[5] B. Redwood, F. Schffer, and B. Garret, *The 3D printing handbook: technologies, design and applications*. 3D Hubs, 2017.

[6] B. Kattel, W. E. Hutchcraft, and R. K. Gordon, "3D printed patch antennas with varying infill densities," in *2023 Antenna Measurement Techniques Association Symposium (AMTA)*, 2023, pp. 1–5. DOI: 10.23919/AMTA58553.2023.10293739.

[7] K. Johnson, M. Zemba, B. P. Conner, *et al.*, "Digital manufacturing of Pathologically-Complex 3D printed antennas," *IEEE Access*, vol. 7, pp. 39 378–39 389, 2019. DOI: 10.1109/ACCESS.2019.2906868.

[8] J. Teniente, J. C. Iriarte, R. Caballero, D. Valcázar, M. Goñi, and A. Martínez, "3-D printed horn antennas and components performance for space and telecommunications," *IEEE Antennas and Wireless Propagation Letters*, vol. 17, no. 11, pp. 2070–2074, 2018. DOI: 10.1109/LAWP.2018.2870098.

[9] Y. Li, L. Ge, J. Wang, *et al.*, "3-D printed high-gain wideband waveguide fed horn antenna arrays for millimeter-wave applications," *IEEE Transactions on Antennas and Propagation*, vol. 67, no. 5, pp. 2868–2877, 2019. DOI: 10.1109/TAP.2019.2899008.

[10] S. Alkaraki and Y. Gao, "mm-Wave low-cost 3D printed MIMO antennas with beam switching capabilities for 5g communication systems," *IEEE Access*, vol. 8, pp. 32 531–32 541, 2020. DOI: 10.1109/ACCESS.2020.2973087.

[11] W. Oropallo and L. A. Piegl, "Ten challenges in 3D printing," *Engineering with Computers*, vol. 32, pp. 135–148, 2016.

[12] K. Günaydın and H. S. Türkmen, "Common FDM 3D printing defects," in *International congress on 3D printing (additive manufacturing) technologies and digital industry*, 2018, pp. 19–21.

[13] T. Nahar and O. Sharma, "Bandwidth enhancement of corportate fed bowtie antenna array operating in l band by changing the substrate material and ground plane length," *International Journal of Computer Applications*, vol. 107, no. 4, pp. 16–19, 2014. DOI: 10.5120/18739-9986.

[14] C. D. Keathley, "Evaluation of manufacturing methods for antenna design," M.S. thesis, The University of Mississippi, 2021.

[15] Voltera. "Voltera conductor 3 ink." (Dec. 13, 2023), [Online]. Available: https://docs.voltera.io/v-one/downloads/technical-data-sheets.

[16] Keysight. "Keysight 85052D 3.5 mm Economy Calibration Kit." (Dec. 13, 2023), [Online]. Available: https://www.keysight.com/us/en/assets/9018-01142/service-manuals/9018-01142.pdf.

[17] B. Kattel, W. E. Hutchcraft, and R. K. Gordon, "Exploring infill patterns on varying infill densities on dielectric properties of 3D printed slabs," in *2023 Antenna Measurement Techniques Association Symposium (AMTA)*, 2023, pp. 1–5. DOI: 10.23919/AMTA58553.2023.10293640.

[18] All3DP. "PEI sheet (3d printing)." (Dec. 13, 2023), [Online]. Available: https://all3dp.com/2/pei-sheet-as-a-3d-printer-print-bed-sheet-a-guide.

[19] J. Ramian, J. Ramian, and D. Dziob, "Thermal deformations of thermoplast during 3D printing: Warping in the case of ABS," *Materials*, vol. 14, no. 22, p. 7070, 2021.

[20] B. Kattel, U. Ayan, M. Mohoppu, B. Villacorta, and W. E. Hutchcraft, "Enhancing permittivity of 3D printing filaments via nanocompounding for electromagnetic applications," in *SoutheastCon 2024*, 2024.